Chapter 22

Fractal Effect of Corrosion on Mechanical Behavior of Unprotected Structural Steel

Francisco Casanova del Angel

Additional information is available at the end of the chapter

http://dx.doi.org/10.5772/57061

1. Introduction

Currently, it is known that, most of the time, the approach to continuous media results are unsatisfactory for use in real materials. In man made structures, defects appear during the production stage at nano-, micro- and macro-scales, which evolve throughout its useful life, generating failures, some of which can be catastrophic. Fractography surveys show the non-Euclidean nature of fracture patterns [1]. Macro-scale breaking patterns are common in experimental laboratory research, while micro- and nano-scale processes, which govern the macroscopic behavior and deformed solids fracture, are not [2].

The fracturing of materials is an interesting problem from a scientific and a technological point of view, which has generated a lot of research regarding the formation and propagation of cracks. It is well established that fracture patterns may be treated from the point of view of fractal geometry [3]. Mandelbrot was one of the main researchers on fractal aspects of metal fracture surfaces. Results obtained on thermally treated steel samples fractured in impact tests suggested a strong correlation between macroscopic tenacity and the fractal dimension of the fracture surface [4]. Currently, it is known that fracture surfaces are fractal objects showing anisotropic scaling. Natural fractals are self-similar (remember that a self-similar object is exactly or approximately similar to a part of itself and in the case of natural fractals, they display self-similar structure over an extended -but finite- scale range), and fracture surfaces are self-similar from a statistical point of view. The self-affine case is described in terms of its parameters, regarding Hurst's exponent or rugosity exponent, ς, and the ξ correlation length, which is the higher limit for which the self-affine behavior is shown.

The fracturing of structures has been a problem since man began to model and build structures. This has become critical, due to complexity of modern structures and heavy operational loads. During the industrial revolution, there was a high increase of metals (iron and steel) usage for

structural applications. Unfortunately, there were also many accidents leading to human and material losses due to failure of such structures. Some of them were due to defective designs, but it has also been discovered that the defects in materials like persistent cracks might have started cracking, thus leading to fracture. The surface of materials depends a lot on properties such as: adhesion, friction, wear, permeability, etc. It is true that surfaces exposed to the environment and interactions between both of them are responsible for the behavior of materials. Data that might be obtained from the surface may be related to microstructure and mechanical properties of material. It must also be remembered that when a metallic piece is under stress, corrosion concentrates causing transgranular or intergranular cracks.

In the specific case of surface fracture, its analysis is usually carried out through metallography, which may tell us about, among others things, the origin of the fracture, the direction of its propagation and the type of load that caused it. The surfaces of fractures are usually a set of repeated patterns, for example, fractures, fissures, ridges, holes and intergranular defects, among others. Quantitative fractography aims at translating such features to a parametrical shape, and that is where fractal geometry comes in [5].

Fractal geometry looks for regularity in the relationship of an object and its parts at various scales, that is, it studies invariable geometrical aspects, regardless of scale changes. In other words, fractal geometry studies non-differentiable or non-continuous geometrical shapes at any scale. From a mathematical point of view, a fractural is a subset of a metric space for which its Hausdorff-Besicovitch dimension is strictly higher than its topological dimension. In general, fractals have some type of similarity and it may be considered that they are made of small parts similar to the whole. This similarity may be strictly geometrical, or only approximate or statistical. Mandelbrot quantitatively explored for the first time, the fractal character of fracture surfaces subject to various thermal treatments and reported a correlation between fractal dimension and tenacity of the fracture, their property estimated through impact energy [4]. These results, though questioned in the beginning, started a new era in the fractography disciplines. From then, analysis of self-affinity of fracture surface is a very active research field, which has had the contribution of modern and sophisticated statistical and mathematical methods.

There are various methods for analyzing self-affinity of fracture surfaces, most of them use profiles extracted from surfaces through the use of experimental techniques. Highly refined experiments, focused on various materials, do not confirm correlation between the fractal dimension and mechanical properties [6]. It has been established that rugosity exponent ζ is the proper parameter by which to describe fracture surfaces in fast kinetic conditions analyzed mainly through scanning electron microscope (SEM). Bouchaud proposed a universal rugosity exponent $\zeta = 0.78$, regardless of microstructure and properties. Such universality was questioned by the discovery of another self-affine regime characterized by a rugosity exponent $\zeta = 0.5$ for fracture surfaces generated in slow crack propagation conditions or analyzed at manometric scales, using atomic force microscope (AFM). Coexistence of both regimes in various materials has also been reported [7]. Such regimes cross in a fracture length, which seems to be independent of kinetic conditions. Attempts to relate such fracture length with microstructural parameters of some materials continue to be carried out. [8]

http://dx.doi.org/10.5772/57061

The development of this research on behavior of unprotected A36 steel exposed to corrosion (the steel had no coating technique applied using zinc as the main protective element), resulted from observing occurrence of cracks on structures exposed to a marine environment, as well as the analysis of consequences implied by such fact, regarding marine corrosion. Research is shown from dimensioning of test specimens; laboratory tests with their chemical analysis; and, finally, a fractography of the corresponding test specimen, obtaining its fractal dimension based on the theoretical development shown.

2. Dimensioning of test specimens

In accordance with ASTM A-370 standard specifications [9] and complying with such parameters (geometrical relationships between length, width and height), Figure 1 shows the type of test specimen used. Table 1 shows proportions for dimensioning of the test specimen used in the laboratory, obtained in accordance with ASTM standards. Test specimens were made of A36 structural steel (C = 0.29 max., Mn = 1.20, Si = 0.40 max., P = 0.40 max., S = 0.05 max). In accordance with ASTM specifications, test specimen were made with A36 structural steel, chemical composition: C = 0.29 max., Mn = 1.20, Si = 0.40 max., P = 0.40 max., S = 0.05 max. Existing Mexican regulations were considered for tensile tests on steel products. [10]

Figure 1. a) Virgin A36 structural steel test specimen, b) after 6 months, and c) after 12 months

Diameter	Diameter in reduced section, D	Radio of transition area, R	Length of reduced section, A
12.0mm± 0.1mm	8.89mm ± 0.17mm	6.35mm± 0.1mm	58.0mm ± 0.1mm

Table 1. Dimension of test specimen to be used in accordance with ASTM A-370 Standard.

3. Laboratory tests and chemical analysis

Tensile tests were carried out in a 250 KN Universal Mechanical Testing machine. Conditions for the test were: testing speed: 0.60 mm/min.; sampling frequency: 5.0 points/s; downwards. Traction assays for unprotected A36 structural steel were carried out on three types of sample, taking into account the base material, and other two samples were applied under real marine corrosion, throughout 6-month and 1-year aging periods, Figures 1.a., 1.b and 1.c. Based on features and components of the metal used, the sample was roughed down and polished in order to remove scratches. The procedure used was the traditional one, consisting in roughing down the surface of the sample and sanding it with an ultimate approximation to a flat surface free from scratches with a moisturized spinning wheel. The sample was moisturized in a Petri dish with a solution of Nital dissolved in water for 10 seconds. Moisturizing time was carefully controlled. Action of moisturizing stopped when the sample was put under a water stream, cleaned with alcohol and a drier was used for finishing [11].

4. Results of mechanical properties of A36 structural steel

A fractographic analysis begins with a final observation of the fracture's surface features. Evidence of nucleation of fissure, mechanism and direction of propagation causes may be obtained, and an estimation of acting loads' magnitude may eventually be obtained. [12] and [13] Figure 2.a shows the results of the stress-strain graph for virgin material (i.e. not exposed to marine conditions), for which a maximum 369.18522 MPa load and a 255.1545 MPa yield strength were obtained. Figure 3.a shows its fractography. For structural steel aged more than 6 months at sea, a 351.50238 MPa maximum load and a 238.676 MPa yield strength were obtained, Figure 2.b. Fractography in Figure 3.b shows nucleated cracks and a behavior ductile to fracture. For structural steel aged more than 1 year, a 315.883 MPa maximum load and a 226.24 MPa yield strength were obtained, Figure 2.c. Fractography shown in Figure 3.c shows crack branching due to tensile testing, since material loses ductility due to corrosion. The second and third columns of Table 2 show the results of the mechanical properties of steel in accordance with the tensile test, and the fourth and fifth columns show specific values of steel regarding the Internet web page referred to [14]. It should be noticed that results obtained from tensile test for virgin A36 structural steel test specimen are very similar to those shown by that Web page.

Stress under which the material changes its behavior from elastic to plastic is not easily detected, so for this reason the yield strength has been determined drawing a line parallel to the starting section of the stress-strain curve, but displaced 0,002 mm/mm (0,2 % from the origin), crossing the curve of the diagram. The intersection point is the yield point.

To obtain fractal dimension of microcracks found in the material, the theoretical description of a fractal's behavior in unprotected A36 steel exposed to corrosion is shown [15].

http://dx.doi.org/10.5772/57061

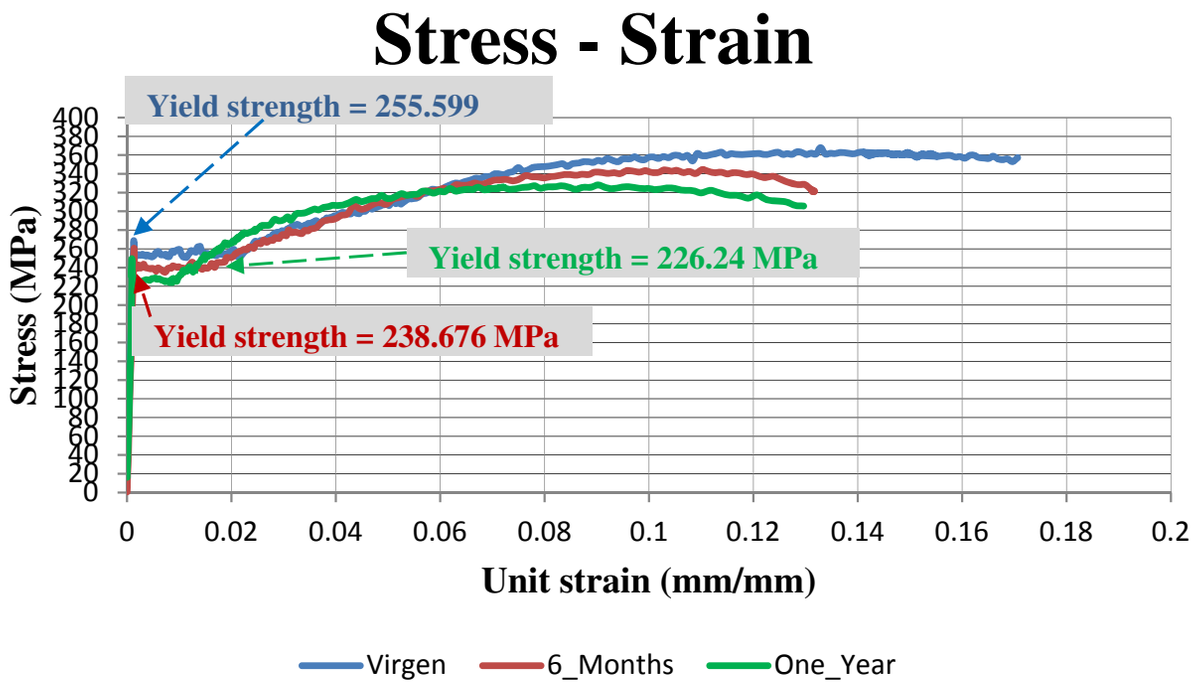

Figure 2. Yield strength for test specimen.

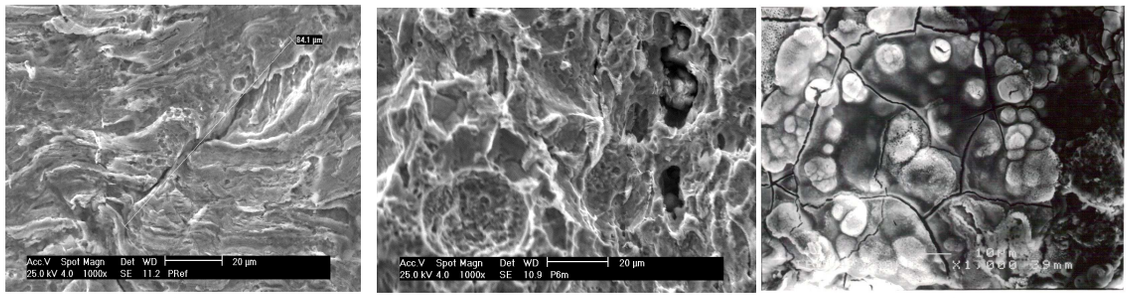

Figure 3. a) Fractography of test specimen. b) Fractography of test specimen after 6 months in marine conditions, and c) Fractography of test specimen after 1 year in marine conditions.

		Tensile test		www.matweb.com	
Material. A36 structural steel	**Yield strength (f_y)**	**Elasticity module (E)**	**Maximum strength**	**Yield strength (f_y)**	**Elasticity module (E)**
Virgin	255.59 MPa	205317.72 MPa	369.185 MPa	250 MPa	200.000 MPa
Exposed 6 months	238.67 MPa	202474.23 MPa	351.502 MPa	X	X
Exposed 1 year	226.24 MPa	198716.21 MPa	315.883 MPa	X	X

Table 2. Mechanical properties of tensile test in accordance with reference [14].

5. A fractal theoretical desciption

Definition of generating curve. Let I_0 be a unitary lenght line segment, contained in a closed interval, that is, $I_0 \subset [a, b]$. Let I_1 be a set with sectioned behavior, consisting in three segments of a straight line which create, based on starting point a of I_0, two scalene triangles reflected regarding the middle point c of I_0, obtained as follows: the first half of segment I_1 is substituted or removed by the sides of triangle which create an angle with I_0. This process is repeated for the second half, but with the sides reflected from middle point c.

This process is known as *generator* which is called state 1. Construction of set I_2 is made applying the generator to every segment of I_1, which is called state 2. Thus, set I_k is created applying generator I_1 on every segment of I_{k-1}, which is called state k, Figure 4.a.

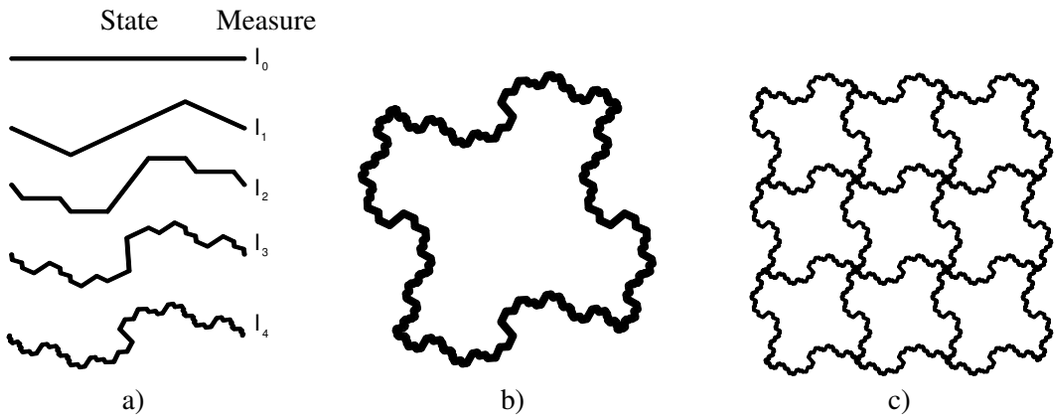

Figure 4. a) Construction of the fractal curve *I*. In every state I_k generator I_1 is applied on every segment of the curve. b) Fractal curve *I* on the plane. c) Fill the plane with the curve fractal.

Somer particular aspects presented in the construction of this type of fractal should be noticed when *generator* is created by combination or triangular layouts (in size and form):

- States I_{k-1} and I_k are different from each other in the sequence shown by poligonal curves $\forall$ $k \to \infty$,
- set I has a fine structure, that is, it contains every detail in every arbitrary small scale.
- although the *generator* is composed by two triangular figures corresponding to euclidean logic, the geometry of I_k $\forall$ $k \to \infty$ is too irregular to be described in classical geometric terms.

Figure 4.b shows the curve built on the plane through reflection of I_k on every side.

Curve I is characterized by being of a similar scale since, based on a transformation F: $\Re^n \to \Re^n$ with $\lambda_i > 0$ $\forall$ i $\exists_n$ $a, b \in \Re^n$ such that $\mid F_i(a)\text{-}F_i(b) \mid = \lambda_i \mid a\text{-}b \mid$. Similarity of scale is present for triangles created with I_0, by generator I_1. In a like manner, it also has the property of being affine, since, based on transformation F already defined, $F(a) = T(a) + \alpha$ with T a non-singular linear transformation and $\alpha \in \Re^n$. It must be remembered that affinity is conceived as a shear

http://dx.doi.org/10.5772/57061

transformation or resistant to cutting, and is a contracting or expanding effect, not necessarily in the same direction. A curve type l_k satisfies the *scale principle* if all its relative figures are linked to each other by a scale law.

Let I be a Borel's set such that $I = \{I_1, I_2, I_3\}$, where I^j is a finite succesion of line segments creating the *generator* $\forall$ j = 1, 2, 3, in order that $I_i = \{U^3_{j=1} I^j_i \ \forall \ i = 1, 2, \dots\}$ is a countable sequence of sets. Thus, measurement μ, of segments I_i is defined as:

$$\mu(U^{\infty}_{j=1} I_i) = \sum^{\infty}_{i=1} \mu(U^{\infty}_{j=1} I^j_i) = \mu(I_i) = 3\mu(I_{i-1}) \ \forall i=1, \quad (1)$$

When a geometrical discontinuity is of the fractal type, generated by a natural process, a uniform reticulate should be built. Let $(\chi, P(\chi), \mu)$ be a space with measures such that the sample space is $\chi = [0, 1]$ and $P(\chi)$ is a set of subsets of χ, where the measurement is μ. Since the system is dynamic, $\chi \subseteq \Re^p$ is the phase space. Let us consider a χ reticulate covered by p-dimensional boxes with radius δ_n, where $B_{\delta n}(t)$ is the neighbor box containing the segment of straight line or point t. Succession of neighbor boxes has radius $\delta_n \rightarrow 0$ as $n \rightarrow \infty$.

Let us suppose that there is subset $I \neq \phi$ from euclidian space n-dimensional, $\Re^n$, and that $|I| = \sup\{|a - b| \text{ such that } a, b \in I\}$. If $\{I_i\}$ is a countable set of neighbors with radius δ covering I, thus, there exists a subset II of $\Re^n$ such that $II \subset (\cup\infty_{i=1} I_i)$ with $|I_i| \in [0, \delta] \ \forall \ i$. Therefore, $\{I_i\}$ is neighbor δ of I. If there is a $k > 0$, then for every neighbor $\delta > 0$ a function to minimze total covering II may be defined as follows:

$$Hk_{\delta}(II) = \inf\left\{\sum \infty_{i=1} | \ I_i \ |^k\right\} \qquad \forall \ \{I_i\} \text{ neighbor } \delta \text{ of } II \quad (2)$$

If in (2) we consider the limit, then lím $H^k_{\delta}(II) = H^k(II)$. It should be taken into account that $H^k(II)$ is known as Hausdorf's k-dimensional measurement.

6. Meshing and definition of fractal outline

Let $N(t^*, \Delta t^*)$ be the number of squares contained by reticulate, and $N(t, \Delta t)$ the number of squares intersected by the fractal curve. $D_{\theta^\circ}(I)$ shall be the fractal dimension, L the total length of the object, and l the length of every segment. Therefore, L/l quotient defines the number of subdivisions contained by every side of the intersected reticulate. These scale properties correspond to a fragmented fractal, and the *multifractal* [16], pp. 45 concept is applied. Based on the above:

$$N(t^*, \ \Delta t^*) \cong \Delta t^* \varrho(t^*) t \ f(t^*) \quad (3)$$

where $t \in [t^*, t^*+\Delta t^*]$. $P(t^*)$ is the probability of distribution of intersection points $t \in [t^*, t^*+\Delta t^*]$ and $f(t^*)$ the fractal dimension of such points.

Considering a random generation of $f(t)$, the original curve is rotated to different angles, preferably constant, in order to calculate D_{θ° for every case.

$$D_{\theta^\circ} = \frac{\sum \left\{ D_{\theta^\circ} \ \forall \ i=1,...,n \right\}}{n} \tag{4}$$

In order to rotate the original curve a certain number of times, let us consider mapping M_n: $\chi \rightarrow \Re$, where $M_n(t) = -\log \mu[B_{\delta n}(t)]$, if $\mu[B_{\delta n}(t)] > 0$ then $C_n(t)$ is a re-scaled version of $M_n(t)$, that is:

$$C_n(t) = \frac{M_n(t)}{-\log \delta_n}$$

where C_n describes the local behavior of μ measurement.

7. Behavior pattern

The fractal behavior of a geometrial discontinuity takes us to the concept of diagonal self-affinity diagonal. In order to define the pattern of the fractal *generator*, let us begin drawing straight lines from its base to the points where such curves are all along its length, and thus obtain a fractioned curve. It is important to draw horizontal lines in case there is a change in its path behavior, in order to identify the affinity along such path.

Horizontal lines identifying the beginning of the generator, must show the feature of proportionality d such that:

$$d = \mathrm{L}\ sen\ \beta \quad \text{where} \quad \operatorname{sen}\beta = L\ /\ d \quad \text{and} \quad \cos\beta = k\ /\ L \tag{5}$$

L is the length of the generator, l the length of every segment, and L/l is the number of subdivisions contained by the *generator*. In order to observe the ideal behavior of the path, the scale relationship is defined as the average of the lengths of adjoining generators, that is, $(L_1 + L_2)/2$; Figure 2.a.

The scale factor of every rotation undergone by the generator or fractal curve, s, is defined as:

$$s = \log_{10}(N) \ \forall N \longrightarrow \infty \tag{6}$$

where the value of N is the average of the highest number of every rotation, that is:

$$N = \sum_{\mathrm{i}} \left\{ R_i \quad \forall \ i = 1,...,n \right\} \tag{7}$$

Based on the above, we may get the scale factor of the generator, defined as the inversion of s which, applied, generates the geometrical structure.

http://dx.doi.org/10.5772/57061

8. Calculation of fractal dimension of the crack for 6-months test specimen

In order to calculate the fractal dimension for cracks generated on test specimen exposed to marine corrosion, both for 6 and 12 months, the theory presented above was applied to fragmented fractals, or fractals generated by natural processes [17]. The original crack was rotated 45°, 90°, 135° and 360° or 0° degrees in order to determine in a more reliable manner the fractal dimension, D_f. The process was to choose a picture for the 6-months test specimen and mesh it in order to calculate its fractal dimension, which is shown in Figures 5.a and 5.b.

In order to obtain fractal dimension D_f, an average of calculated dimensions for each of the four rotations applied to the fractal curve was obtained. Fractal dimension for a crack on structural steel exposed 6-months to marine conditions is:

$$D_f = (D_{0°} + D_{45°} + D_{90°} + D_{135°})/4 = (1.34950+1.3429+1.3398+1.3432)/4 = 1.34385$$

In order to verify that fractal dimension calculated under the theory developed above is valid, the commercial software *Benoit* was used. The fractal dimension obtained with such program is $D_f = 1.34029$ [18]. As may be seen, the results are similar.

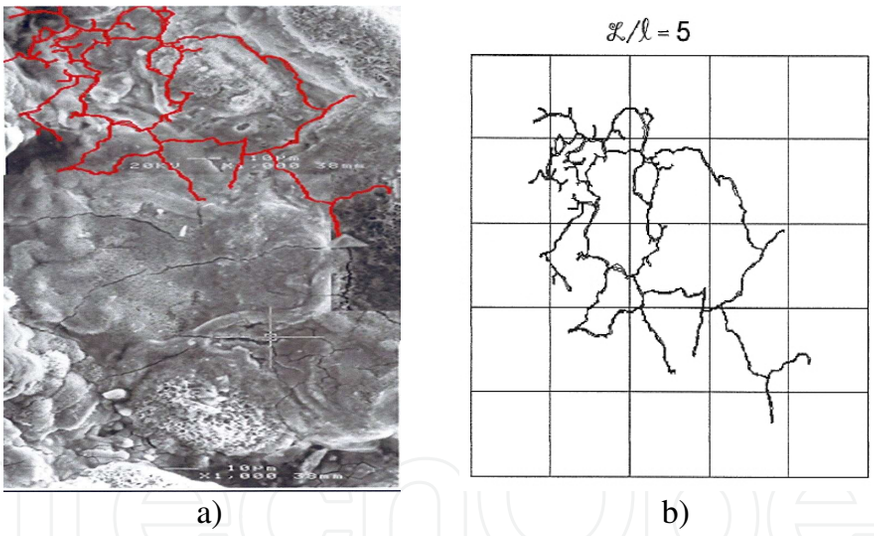

Figure 5. a) Fractal behavior of the crack for 6-month test specimen. b) Meshing of fractal with 5 subdivisions and 0 degree rotation.

9. Calculation of fractal dimension of the crack for 1-year test specimen

Figure 6.a shows fractal behavior of the crack, and Figure 6.b shows its digitalization. To obtain fractal dimension of the 1-year test specimen in marine conditions, the same calculation procedure used for the 6-month test specimen was carried out.

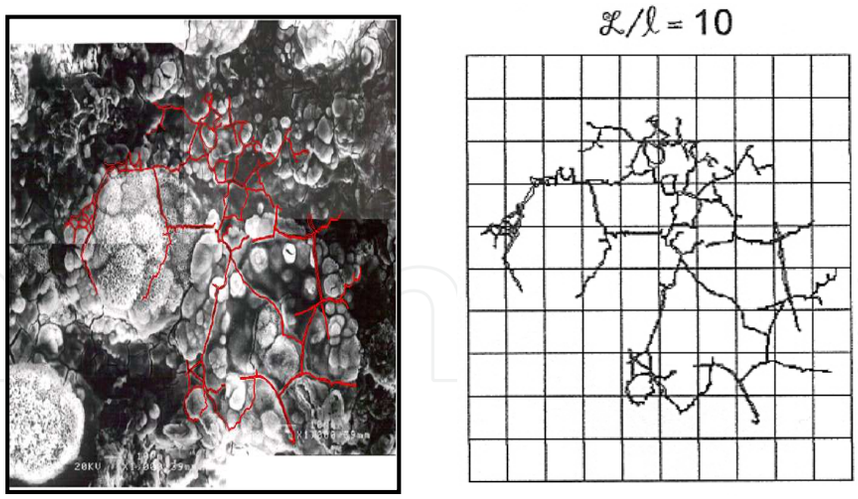

Figure 6. a) Fractal behavior of the crack for 1-year test specimen. b) Meshing of fractal with 10 subdivisions.

Fractal dimension for a crack in A36 structural steel exposed to marine conditions throughout a year is as follows:

$D_f = (D_{0°} + D_{45°} + D_{90°} + D_{135°})/4 = (1.3946+1.3943+1.4+1.3943)/4 = 1.3958$

That is, fractal dimension of the cracks in A36 structural steel exposed to marine conditions throughout a year has a 1.3958 value. In accordance with *Benoit* commercial software, its fractal dimension is 1.40040 [18].

10. Microanalysis

The X-ray microanalysis study on test specimen aged 12-months at sea shows presence of carbon, oxygen, iron, silica, sulphur, chloride, sodium, calcium and magnesium as the most representative elements, Figure 7. Chloride linked to sodium; basic constituents of sea water, are present as sodium chloride. Magnesium is present in constant relation with chloride which, when combined with other elements, creates magnesium chloride and magnesium sulfate. Sulphur is present in sulphates. All these elements have made possible acceleration of test specimen's corrosion.

11. Discussion of results

Virgin A36 structural steel showed a ductile fracture surface, which caused concentration of stresses and a local increase of plastic deformation. The elements showed uniform corrosion for both cases of marine exposition, which caused a generalized thinning on the entire surface. They also showed pitting corrosion and a fragile and porous surface.

http://dx.doi.org/10.5772/57061

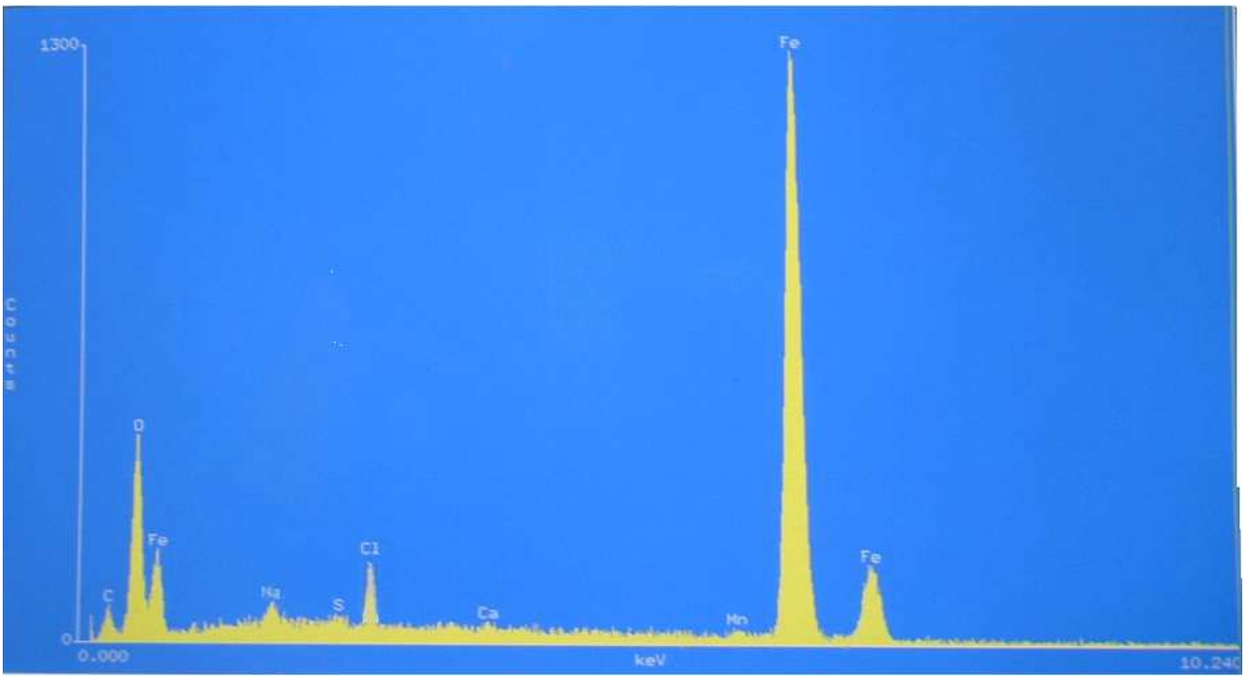

Figure 7. Analysis spectrum through electron microscopy.

A loss of ductility of 11.96 % (6 months) and 43.87 % (12 months) were recorded after marine exposition, regarding the virgin test specimen. These small values do not allow creation of a function for loss of ductility due to permanence of steel in Pacific Ocean coasts. This loss of ductility is mainly attributed to the presence of hydrogen, an element present in sea water and organic compounds on the site of marine exposition, causing it to be absorbed and transported to the inside, towards imperfections of the element, thus causing separation of grain borders.

In the case of tensile tests, breaking had to be achieved in order to calculate the fractal dimension of crack generated. The corresponding stress-strain graphical expression shows variation in the fluency strength in each exposition, due to the reduction of the area based on type of uniform corrosion found.

Once the crack was obtained, it was digitalized and the description format to obtain its fractal type was applied. Then, it was verified that such generator was applicable to fractal behavior of the crack. This being so, the crack was meshed, subdivided and rotated at various angles for calculation of its fractal dimension. Fractal dimension calculated shows a ± 0.0036 variation regarding commercial software, which may be due to the box counting algorithm. Fractal dimension obtained for the test specimen exposed 12 months at sea shows a fractal dimension higher than the 6-month test specimen, since the crack has more branches.

12. Conclusions

Regarding exposition of probes to the environment, it may be affirmed that, due to interaction of an alloy with the environment to which it was exposed, corrosion products were generated

on it, which changed failure mechanism of probes subject to tensile assay. Probes exposed on both periods have significant stress concentrations on areas where corrosion developed. This was observed in laboratory assays, since failure appeared in such areas.

Regarding theoretical development of fractals obtained, it has been carried out from line segments creating a generating curve characterized by sets of Borel's theory, which is possible since generation of fractal curve is carried out through natural processes generating geometrical discontinuities of any typical fractal. Characterization of fractal is carried out on a reticulation and its value is based on count of segments for every box in such reticulation. The original crack was rotated 45°, 90°, 135° and 360° or 0° degrees in order to determine in a more reliable manner the fractal dimension, D_f. Self-affinity of the fractal is also tested.

Fractal dimension obtained after six months of exposition is lower regarding that obtained at 12 months, which shows that exposure time is directly proportional to cracks generated due to corrosion products and that crack ramification influences the corresponding value.

Acknowledgements

This document and its corresponding research was carried out, in part, with research Project IPN-SIP 20120585. Thanks to the Martín Armando Zamora García, M.Sc., for allowing the use of photographs used.

Author details

Francisco Casanova del Angel*

Address all correspondence to: fcasanova@ipn.mx; fcasanova49@prodigy.net.mx

SEPI of the ESIA, Unit ALM of the IPN, Mexico

References

[1] Cherepanov G. P and Balankin, A. S. 1997. Fractal and Fracture. A topical encyclopedia of current knowledge dedicated to Alan Arnold Griffith, G.P Cherepanov E.D., Krieger, Melbourne, pp. 104.

[2] Izotov, A. D, Balankin S and Lazarev V. 1993. Synergetics and Fractal Thermomechanics of Inorganic Materials. II. Fractal Geometry of Fracture in Solids. Inorganic Materials. Volume 29, No. 7, pp. 769-778.

[3] Caldarelli G., C. Castellano and Vespignani. 1994. Fractal and topological properties of directed fracture. Phys. Rev. E. E, 49 number 4, pp. 2673-2679. URL: http://

link.aps.org/doi/ 10.1103/PhysRevE.49.2673. Doi: 10.1103/PhysRevE.49.2673. PACS: 64.60.Ak, 62.20.Mk, 05.40.+j.

[4] Mandelbrot B. B. 1982. The Fractal Geometry of Nature. Freeman, New Cork, pp. 459. ISBN-13: 978-0716711865.

[5] Ipohorski, M. 1988. Fractografía-Aplicación al análisis de falla. Informe CNEA 490. Buenos Aires, Argentina.

[6] Bouchaud, E. 1997. Scaling Properties of Cracks. Journal of Physics: Condensed Matter. Volume 9, Number 21, pp. 4319-4344. ISSN: 1361-648X (Online). Doi: 10.1088/0953-8984/9/21/002

[7] Daguier P, Hénaux S, Bouchaud E and Creuzet F. 1996. Quantitative Analysis of a Fracture Surface by Atomic Force Microscopy. Phys. Rev. E, 53, 5637.

[8] Daguier P and Nghiem B. 1997. Pinning and Depinning of Crack Fronts in Heterogeneus Materials. Phys. Rev Left. Volume 78, Issue 6, pp. 1062. URL:http:// link.aps.org/doi/10.1103/ PhysRev Lett. 78.1062. Doi: 10.1103/ PhysRevLett.78.1062. PACS: 62.20.Mk, 05.40.+j,81. 40.Np.

[9] ASTM A-370. Standard Testy Method and Definition for Mechanical Testing of Steel Products. CFR Sections(s): 49 CFR 179.102-1(a)(1). American Society for Testing and Materials.

[10] NMX-B-310-1981. 1996. Métodos de prueba a la tensión para productos de acero. Secretaría de Comercio y Fomento Industrial. México. Norma Mexicana.

[11] Dowling, A. R and Townley, C. H. A. 1975. The effects of defects on structural failure: A two criteria Approch. International Journal of Pressure Vessel and Piping. Vol. 3 pp. 77-107. http://dx.doi.org/10.1016/0308-0161(75)90014-9

[12] Handbook ASM. 1987. Fractography. The Metals Information Society. Former Ninth Edition, Vol. 12.

[13] Roylance D. 2001. Introduction to Fracture Mechanics. Department of Materials Science and Engineering. Massachusetts Institute of Technology. Cambridge, MA. 02139.

[14] Web paged consulted and referred to in the text. http.//www.matweb.con/index. February 2012.

[15] Cortés P. R, Villanueva A. J, Ponce L. E, Rojas M. M and Rojas Z. E. 2004. Estudio de la soldabilidad y corrosión del acero inoxidable AISI 904L con los agentes utilizados en la lixiviación del cobre. Revista Facultad de Ingeniería de la Universidad de Tarapacá. Vol. 12 N°2, pp. 43-56. http://dx.doi.org/10.4067/S0718-13372 004000 200007.

[16] Mandelbrot B. B. 1997. Fractales, hasard et finance. Paris: Ed. Flammarion. ISBN: 2-08-08132-X.

[17] Bouchaud E, Lapasset G and Planès J. 1990. Fractal Dimension of Fracture Surfaces: A Universal Value?. EPL (Europhysics Letters). Vol. 3, No. 1. pp. 73. ISSN: 1286-4854 (online). Doi: 10.1209/0295-S075/13/1/013.

[18] Benoit – Fractal Analysis Software. 2012. www.trusoft.international.com/

[19] Arteaga A. J. 2005. Análisis de micro Fracture. Tesis de Maestría. SEPI-ESIA Zacatenco, IPN, México.

[20] Burdekin, F. M and Dawes, M. G. 1971. Practical Use of Linear Elastic and Yielding Fracture Mechanics with Particular Reference to Pressure Vessels. Proceedings of the Institute of Mechanical Engineer Conference, London, pp. 38-37.

[21] Budiman, H. T and Lagace, P. A. 1997. Non Dimensional Parameters for Geometric Nonlinear Effects in Pressurized Cylindrical with Axial Cracks. Transaction of ASME, Journal of Applied Mechanics, Vol.67.

[22] Chaaban, A and Ahaarani, A. 1991. A Proponed K1 Solution for Long Surface Cracks in Complex Geometries. Transaction of the ASME, Journal of Pressure Vessel Technology.

[23] Cherepanov G. P and Balankin, A. S. 1995. Fractal Fracture Mechanics. Eng. Fract. Mech., 51, pp. 997-1033.

[24] Folias, E. S. 1965. An Axial Cracks in Pressurized Cylindrical Shells. "International Journal of Fracture Mechanics", Vol. 1 N° 2, 104-113.

[25] González Velázquez J. L. 2000. Impacto en el análisis de integridad en el mantenimiento de ductos. Revistas Academia; pp, 7-13.

[26] González V. 1998. Mecánica de fractura bases y aplicación. Editorial Limusa.

[27] Harrison R. P, Loosemore. K. Milene, I and Dowling, A. R. 1980. Assessment of the integrity of structures Containing Defects. Central Electricity Generating Board Report R/H/R6-Rev2.

[28] Hinojosa M, Bouchaud E and Nghiem B. 1999. Materials Research Society Symposium Proceedings. Volume 539. Materials Research Society, Warrendale Pennsylvania. pp. 203-208.

[29] Irwin, G. R. 1948. Fracture Dynamics. Fracture of Metals. American Society for Metals. Cleveland, pp. 147-166.

[30] Newman, R. C. and Procter, R. P. M. 1990. Stress Corrosion Cracking. Journal British Corrosion Cracking. Vol. 25, N°. 4, pp. 259-269. Doi: http://dx.doi.org/ 10.11 79/00070599156 373.

[31] Rice, J. R. 1968. A Path Independent Integral and the Approximate Analysis of Straing Concentrations by Notches and Crack Problems. Journal of Applied Mechanics, Vol. 35, pp. 379-386. Doi: 10.1115/1.3601206

[32] Timoschenko Gere. 1986. Mecánica de materiales. Editorial Iberoamericana.

[33] Westergaard, H. M. 1939. Bearing Pressures and Cracks. Transaction, ASME, Journal of Applied Mechanics, A, 49, June.

[34] Wells, A. A. 1955. The Condition of Fast Fracture in Aluminum Alloys with Particular Reference to Comet Failures. British Welding Research Association Report.

[35] Wells, A. A. 1963. Application or Fracture Mechanics at and Beyond General Yielding. British Welding Journal. Vol. 10, pp. 563-570.

[36] Winne, D. H. and Wundt, B. M. 1958. Application of the Griffith Irwin Theory of Crack Propagation to the Bursting Behavior of Disk, Including Analytical and Experimental Studies. Transactions of the American Society of Mechanical Engineers, Vol. 20. pp. 1643-1655. ASME.

IntechOpen